Proceedings of the 39th IAHR World Congress
19-24 June
2022 Granada, Spain

Physically Based Vulnerability Functions for flood risk mapping in mountain area

Marco Pilotti(1), Gabriele Farina(2), Riccardo Bonomelli(3), Luca Milanesi(4)

[1] University of Brescia, Brescia, Italy, marco.pilotti@unibs.it
[2] University of Brescia, Brescia, Italy, g.farina008@unibs.it
[3]University of Brescia, Brescia, Italy, r.bonomelli@unibs.it
[4]University of Brescia, Brescia, Italy, luca.milanesi@unibs.it

Abstract

The development of physically-based vulnerability functions is of paramount importance for providing a reliable estimate of flood-related risk. To this purpose, we believe that the vulnerability of human life must be considered as the dominant priority in the production of risk maps whenever the flood warning time is short with respect to the time of implementation of civil protection measures. This situation is typical of mountain areas. In this contribution we present a comprehensive example of flood risk maps computation for a test case in the floodplain of a mountain area in the Italian alps. The example is based on some physically based approaches that we have proposed in the literature to compute the vulnerability of people, cars and masonry buildings that, in turn, are linked to human life.

Keywords: Flood risk assessment, Mitigation and adaptation measures, Shallow water equations, Numerical simulation.

1. INTRODUCTION

Although floods are unavoidable natural phenomena, the *a priori* evaluation of flood risk should lead to the prevention, protection and preparedness against flood adverse consequences for human life, cultural heritage, economic activity, infrastructure and the environment. Accordingly, the European legislation (DIRECTIVE 2007/60/EC) requires the preparation and periodic updating of flood hazard and risk maps in correspondence of low, medium and high probability flood events.

Whereas there is fundamental agreement on the procedure to compute hazard maps through the use of suitable mathematical models (e.g., the Shallow Water Equations) and the quality level that can be obtained is potentially very good, the same is still not true for the computation of risk. In this area there is not a single well-recognized methodology. The reason is that the computation of risk requires the identification of goods at stake and of their vulnerability. These goods have different natures and the potential damage caused by a flood (their vulnerability) is not describable by a single metric. Accordingly, apart from the difficulty of computing vulnerability, damages suffered by different exposed elements cannot be easily summed. This weakness is made even more striking if one considers that the economic and social implications of risk mapping can be huge and would demand assessment criteria that are based on crude conceptualizations.

The DIRECTIVE 2007/60/EC shows a clear hierarchy when it considers the indicative number of inhabitants potentially affected, as a first indicator of the flood's adverse consequences. However, whereas there is no doubt that life is the first priority, in real cases it can be difficult to interpret this indication, e.g. in situations where a long flood warning is possible and where, on the other hand, non-relocable important economic assets are presents. In these cases, probably the priority could be reversed and the metric could be purely economic.

On the other extreme, we believe that the vulnerability of human life must be considered as the dominant priority in the production of risk maps whenever the flood warning time is short with respect to the time of implementation of civil protection measures. This situation is typical of mountain areas, which are typically characterized by impulsive events, such as flash floods or debris flow. Flash floods may be triggered by high-intensity rainfalls or by dam-break/dam-breach events with potentially catastrophic consequences on the downstream areas. However, it can be typical also of situations where the hazard is caused by unforeseen residual events such as a levee breach of a river during a flood.

In such situations flood risk computation be considerably simplified because it is based on a single dominant asset. On the other hand, even in this simpler situation where there is no need of resorting to multicriteria analysis, one has to give meaning to the word “affected”, by providing a metric for the impact of a flood on a

©2022 IAHR. Used with permission / ISSN-L 2521-7119

human being. In this contribution we argue that a way to measure this impact is by measuring the physical vulnerability of people to floods. But how to measure vulnerability? Often this is done simply on the basis of the local population density, so confounding the concept of vulnerability with that of exposure.
In our past research (e.g., Milanesi et al., 2015, Milanesi and Pilotti, 2019) we made the simple (but not simplistic) assumption that a loss of stability of a person impacted by flow, and potentially dragged away, could be used as a metric of human vulnerability. The stability of people impacted by flow has long been considered in the past (e.g., Jonkman and Penning-Rowsell, 2008, Foster and Cox, 1977) but no simple and general model was provided.
An effective model to compute the limiting stability conditions of a person impacted by a flow was proposed by Milanesi et al. (2015, 2016) who conceptualized the human body as a set of cylinders, placed on a slope and impacted by a flow of given depth, velocity and density. The stability condition was defined by coupling equilibrium conditions to slipping, toppling and drowning.
The evidence of past floods also shows that, at least in urban areas, people frequently die trapped in cars that are dragged away by the flow. Accordingly, a similar physically-based approach was proposed by Milanesi and Pilotti (2019) to assess the stability of vehicles impacted by a flow. In this case, the geometry of the car is considered as a watertight squared prism at a fixed distance from the ground. The main novelty of this model was the capability to calibrate, from literature experimental data, a set of hydrodynamic parameters representative of the average stability conditions of a wide range of circulating vehicles.
During extreme events also the building stability could be challenged and human vulnerability can be computed also for the built environment. An example, a physically-based model to assess the stability of masonry buildings with load-bearing walls (Milanesi et al., 2018) allowed to define dimensionless charts for the maximum water depth that can be supported by the building before collapsing as a function of its geometrical and structural configuration. However, our proposed criteria are valid only for masonry building and, accordingly, will not be considered in the following. In this contribution we present an application of risk mapping along a reach of the Oglio river in an alpine valley located in northern Italy, based on the first two mentioned criteria. After computing the hydraulic hazard by the solution of SWE, the depth and velocity maps are used for the computation of human vulnerability. Eventually, the information on population density is used to provide a comprehensive and physically-based map of flood risk.

2. METHODS

2.1 The computation of hydraulic related risk

According to Varnes (1984), the overall degree of loss due to a particular natural phenomenon, or total Risk R, is the logical product of Hazard H, the probability of occurrence at a point and within a given return period of a potentially damaging phenomenon; the Vulnerability V, the degree of loss to a given element at risk, resulting from the occurrence of the hazard; the overall number of exposed elements, E. Symbolically, one can write:

$$R = H \times V \times E \quad [1]$$

In correspondence of a given hydrologic event with known return period, the hydraulic hazard is provided by a suitable function of water depth and velocity during the event. The rational way to compute the depth and velocity is by suitable modeling of the process. In the following the 2D flood simulation was modeled with HEC-RAS 2D, implementing the full momentum form of the Saint-Venant equations.
Exposure (E) is the simpler information to get and it is provided by information on the density of population within each subarea that makes up the investigated area. According to the Italian administrative system, the population is periodically counted for a set of elementary units called census blocks. To give an idea, in the area of the considered test case the average area of these units is 0.87 km^2, ranging between 8000 m^2 and 16.64 km^2 as a function of urbanization, census block may be large in rural and remote areas. Although it is evident that people can move everywhere on the flooded domain, it is reasonable to give a higher level of probability of people's presence to the area where the population density is maximum. After a suitable normalization, the exposure can range between 0 and 1.

2.2 Computation of the vulnerability of people

The vulnerability model proposed by Milanesi et al. (2015) provides the stability of a person impacted by a flow through a physically based approach that includes the role of sloping terrain and of fluid density. The model is based on a limited set of parameters describing the geometry of the body and its hydrodynamic interactions

©2022 IAHR. Used with permission / ISSN-L 2521-7119

with the flow. These parameters have been retrieved from the literature so that the model is weakly parametric. Only the friction coefficient required a calibration based on literature experimental data. To our knowledge, the resulting thresholds, which were computed on the basis of the body size of average European adults and children but can be specialized on the basis of the typical body size of other areas worldwide, provide the best fit with the available experimental data in the literature.
In the model the interaction between the flow and the person is based on the analytical representation of the components of its submerged portion (i.e. frontal area, volume, the center of mass) as a function of the water depth h (m). After schematizing the human body as a set of cylinders, all the forces involved in the balance, namely weight, buoyancy, friction, drag, and lift, can be easily computed. Assuming that human safety in a flow is guaranteed by static stability, the failure mechanisms considered in the model are slipping and toppling, modeled by the equilibrium of forces in the direction of the flow and by a moment equilibrium around a pivot point (i.e. the heel), respectively. Additionally, a condition based on a maximum flow depth independent from the velocity was added to account for the vulnerability to drowning. Finally, the 3 resulting stability thresholds can be considered together, in order to find out the minimum admissible water depth for each given flow velocity, as a function of the flow density and of the local slope. Figure 1 shows the three different failure mechanisms and the resulting combination. Two vulnerability curves are shown: the upper one is valid for an average European adult and the lower one for an average European 7 years old child.

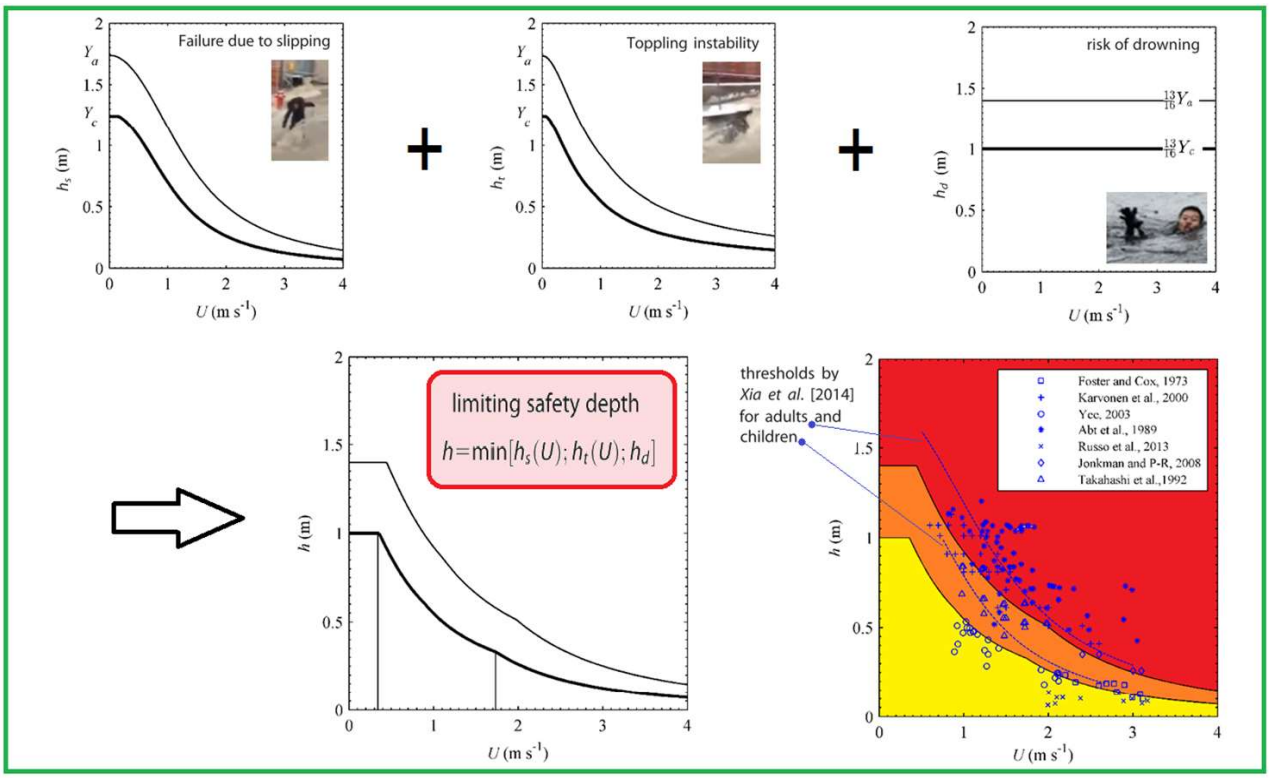

Figure 1. Vulnerability functions for slipping, toppling, drowning, their combination and a comparison with available literature data from physical experiments.

For the case of water on a horizontal slope, two easy-to-use operational formulations of these thresholds can be obtained through interpolation as

$$h_{adults} = \min\left(1.4; \frac{2.809}{U+1.102} - 0.416\right) \quad [2]$$

$$h_{children} = \min\left(1; \frac{1.565}{U+0.884} - 0.275\right) \quad [3]$$

2.3 Computation of the vulnerability of cars

Vehicles impacted by a flow may lose stability becoming hazardous for both occupants and pedestrians. Often people drown within cars that are dragged in areas of deep water. Accordingly, the assessment of vehicles stability in a flood can be regarded as an additional criterion to assess people safety.
Milanesi and Pilotti (2019) proposed a conceptual stability model for a stationary vehicle impacted by a flow accounting explicitly for the role of fluid density and of the sloping terrain. The model, that considered the vehicle as a square body properly elevated from the terrain, considered the equilibrium to slipping and was written in a dimensionless form in order to calibrate a set of hydrodynamic coefficients of lift and drag representative not only of a single vehicle, as customary in most of the literature studies, but of the overall vehicles tested in laboratory conditions.

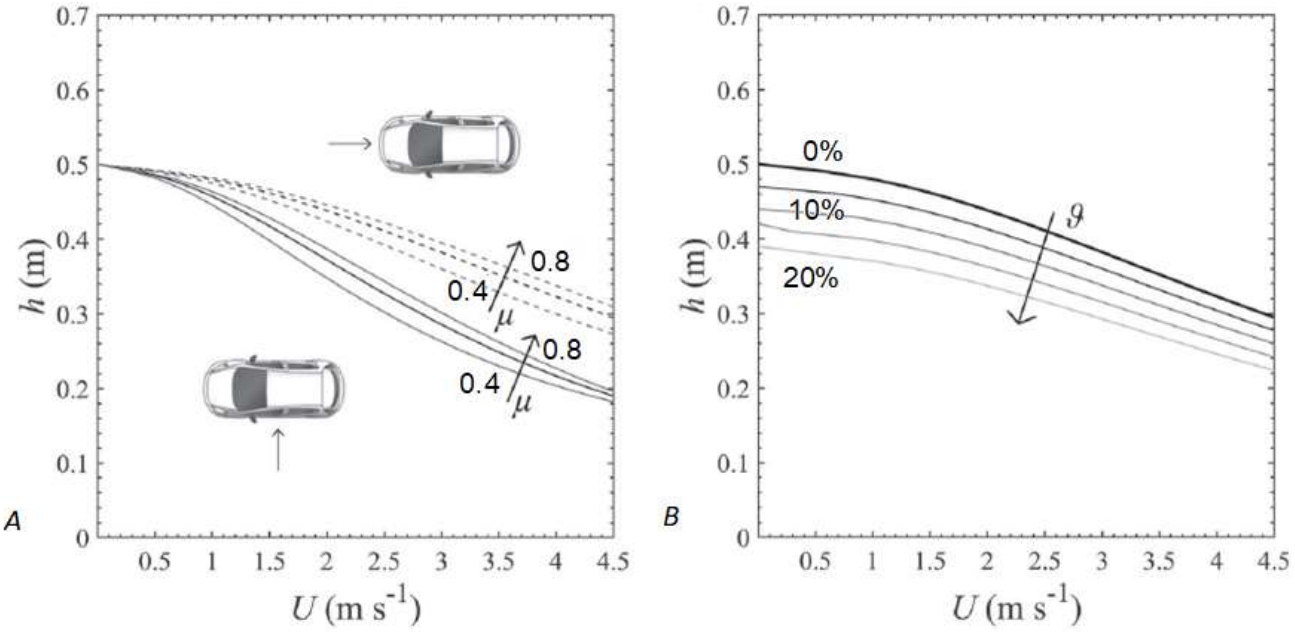

Figure 2. (A) Stability thresholds for an average European vehicle impacted by flow in parallel (dashed lines) and perpendicular (continuous lines) direction and sensitivity of the curves to the friction coefficient. (B) Stability thresholds for the average European vehicle impacted by flow in parallel direction and sensitivity of the curves to the local slope.

In addition to the hydrodynamic coefficients, the model requires basic geometric data representing the size of the vehicle (i.e. length, width, weight, ground clearance, etc.) and the friction coefficient that can be easily selected in narrow literature ranges.
Both the dimensionless and the dimensional forms of the model provided the best available fit to the measured stability limits of each tested vehicle. In addition, stability thresholds based on the calibrated hydrodynamic coefficients and on the average dimensions of the European circulating vehicles were provided. These thresholds, being representative of the stability conditions of a typical vehicle circulating in Europe, can prove particularly useful for practical application. Two easy to use approximate formulations of the stability limit as a function of the flow velocity depth h and of the local slope ϑ are given, for parallel and perpendicular relative orientation of the flow respectively, as:

$$U \le \left[\frac{(604 - 685\tan\vartheta - 1218h)\cos\vartheta}{38h + 1} \right]^{1/2} \quad [4]$$

$$U \le \left[\frac{(390 - 443\tan\vartheta - 788h)\cos\vartheta}{68h - 1} \right]^{1/2} \quad [5]$$

Equations 4 and 5 are defined for 0.158 <h< hb ≈ 0.495 m, where hb is the depth at which the vehicle starts floating in static water. Considering that the stability threshold for stationary vehicles impacted by a flow in perpendicular orientation is more cautionary than the case of parallel direction, eq. [5] only will be considered in the following analyses.

©2022 IAHR. Used with permission / ISSN-L 2521-7119

2.4 Combined use of thresholds

The stability threshold for people and for vehicles provided by eqs. [2], [3] and [5] can be easily combined to produce a vulnerability mapping with zones of growing risk. For instance, in a five-level grading, they go from white (no vulnerability at all, point (0,0) in Figure 3) to dark purple (maximum vulnerability) through yellow, orange and red. The V4 zone corresponds to areas where adult people life is clearly challenged. The V3 zone corresponds to areas where children life is challenged. The V2 zone corresponds to areas where children are safe but not people in cars. Finally, the V1 zone corresponds to areas where people in cars are safe.

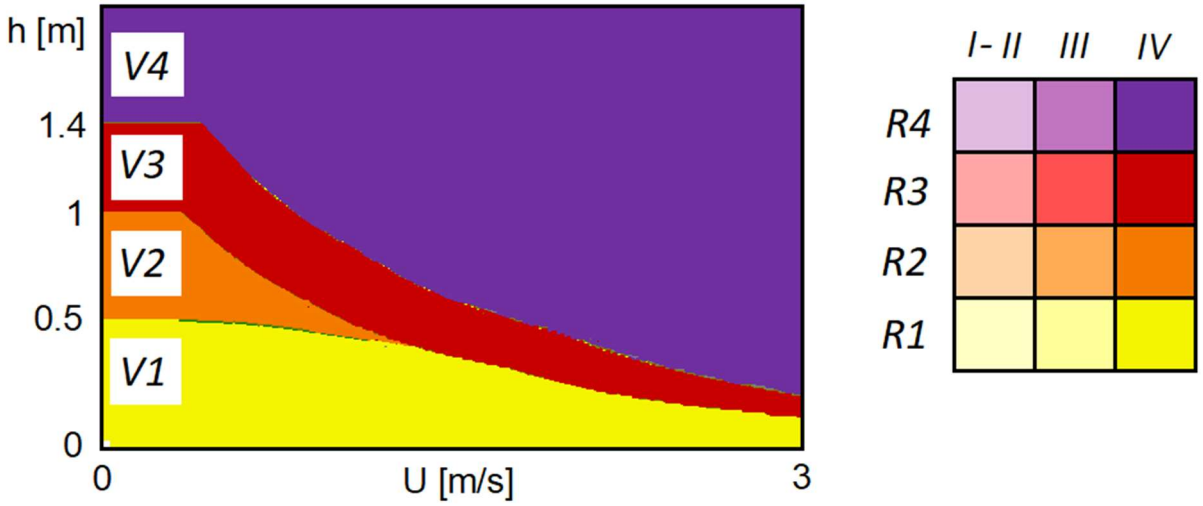

Figure 3. Combined stability thresholds for people and cars. See text for explanation of labels

The informative content of a map classified with the threshold of Figure 3 can be representative of risk if the density of population, as a metric of exposure, is known. In such a case, considering that any risk grading must be relative, the density quartiles in the investigated areas can be computed and a color grid that combines vulnerability with exposure can be easily built as shown on the right side of Figure 3. Here the roman numbers correspond to the population density quartiles. In this way, a map with 5 colors but with 12+1 (white) different levels of risk can be easily built, as shown in the following example. It is here important to underline that the criterion shown in Figure 3 should be applied at each time step of the SWE simulation to each point, keeping in memory the maximum risk value to be mapped in the final risk representation. However, this can be done only when a proprietary SWE code is available. Actually, SWE commercial solvers usually provide the maps of maximum water depth and velocity during the simulation and the use of these two maps, as customary in most applications, leads to a more cautionary classification of risk since the maximum values of flow depth and velocity might occur at different times during the event. For instance, during the filling of a cavity, the maximum velocity occurs during the initial part of the event whereas the maximum depth is reached at the end, when the cavity is full and the velocity progressively goes to zero.

3. THE TEST CASE OF CIVIDATE-DARFO

In the following the proposed procedure will be applied to the reach of the Oglio river between the villages of Cividate and Darfo, in the alpine Valle Camonica, northern Italy. In this 15.29 km long stretch, the risk mapping activities prescribed by the DIRECTIVE 2007/60/EC identified, in correspondence of a river discharge of 995 (1141) m^3/s with a return period of 200 (500) years, floodings caused by a hypothetical breach of the left levee in a point where the same event happened during the challenging 1960 flood. The flooded area is a floodplain inhabited by 6275 people and with relevant economic activities.
In the following (see Figure 4) a first map of the flood risk for people is obtained simply considering the flooded areas as a metric of hazard and the density of population as a metric of vulnerability and exposure. Five color shadings are obtained on the basis of the population density: they go from white (unpopulated zones), yellow (I quartile) , orange (II quartile), red (III quartile), and dark purple (IV quartile). Clearly this type of representation, based only on exposure and leveling hazard on a single on/off grade, provides a zero-order approximation to the concept of risk provided by eq. (1). For instance, urban flooding with very low water depth, happening in an area of high population density, would show up as characterized by maximum risk, whereas very dangerous debris flow on a relatively unpopulated alluvial fan would be downgraded to low-risk areas.

An improved map (see Figure 5) is obtained by implementing the proposed approach of Figure 3. Figure 5 is obtained by locally computing the risk index with the spatial resolution provided by the hazard map, and then by averaging the obtained classification on the census blocks.

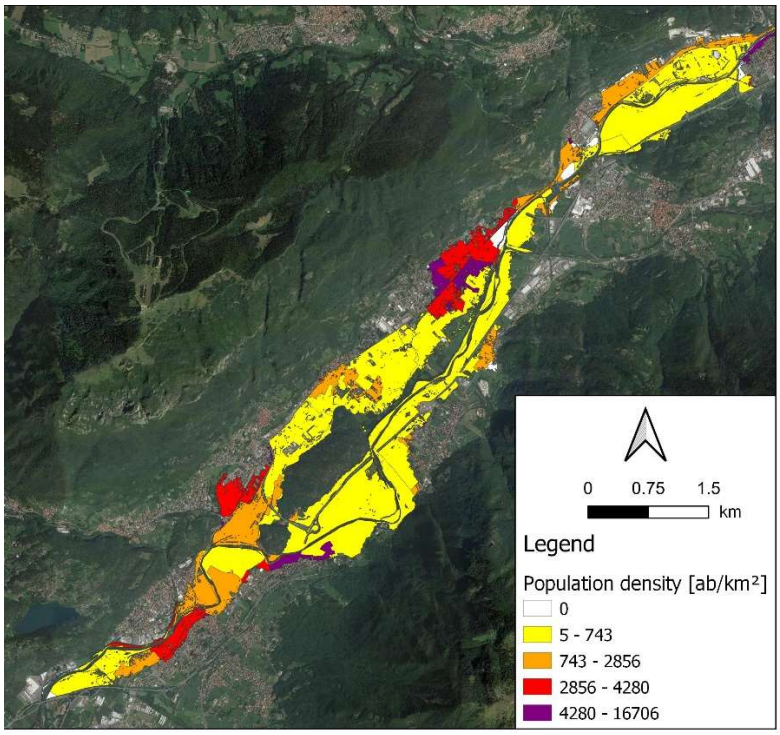

Figure 4. Risk map based on density quartiles of population in flooded areas.

The flood risk map obtained using the proposed approach provides an informative content that is comprehensive of three fundamental aspects:

- first, it is local, being based on the information provided by a SWE solver, whose resolution is typically proportional to the spatial resolution used for the bathymetric description. Although with the increasing availability of LIDAR survey cellsize can be easily smaller than 1m, it is however advisable to average spatially the result of the vulnerability to decrease the level of space scattering of the representation. To the other extreme, the areal averaging on the census blocks prescribed by Italian law downgrades the spatial variability represented by the described method and could hide areas of high risk.
- Second, the method takes into account the density of the population in each area. This is a very important piece of information: if the life of one thousand people is at risk, the probability of an actual casualty is certainly higher than when 10 people undergo the same level of hazard.
- Third and most important, it is based on a clear physical criterion: it uses the physical information provided by the solution of SWE synthesized through a clear metric of the physical challenge exerted by the flood on the involved people

If, for some particular reason the information on local velocity is not provided, such as when the flood extent is obtained through a 1D simulation that provides only the average velocity on the cross-section, the criterion can be used in terms of water depth only. In such a case, the resulting map is shown in Figure 6. Considering the criterion shown in Figure 3, the use of water depth only tends to underestimate the risk, as can be observed in the considered test case (see Figures 5 and 6). This underlines the added value provided by the velocity maps, that are usually an ordinary fallout of 2D SWE simulations.

4. CONCLUSION

Flood hazard and risk maps are important instruments dictated by national agencies for land use planning and emergency management. Considering the strong economic implications of the constraints descending from these tools, risk assessment requires the most rational quantitative approaches available.
Focusing on rapidly evolving floods that usually affect mountain basins, we argue that, due to the high damaging potential of such processes and the insufficient time frame for a safe evacuation of the population, in these areas the targets to be considered in risk assessment is mainly people safety, contrary to economic damages

©2022 IAHR. Used with permission / ISSN-L 2521-7119

that are prevailing in case of slowly evolving floods. We show an example of risk mapping in an alpine valley of northern Italy, using physically based criteria that provide a clear metric for the risk for the life of people impacted by flow. The computed maps concentrate three levels of information: the water depth and velocity provided by

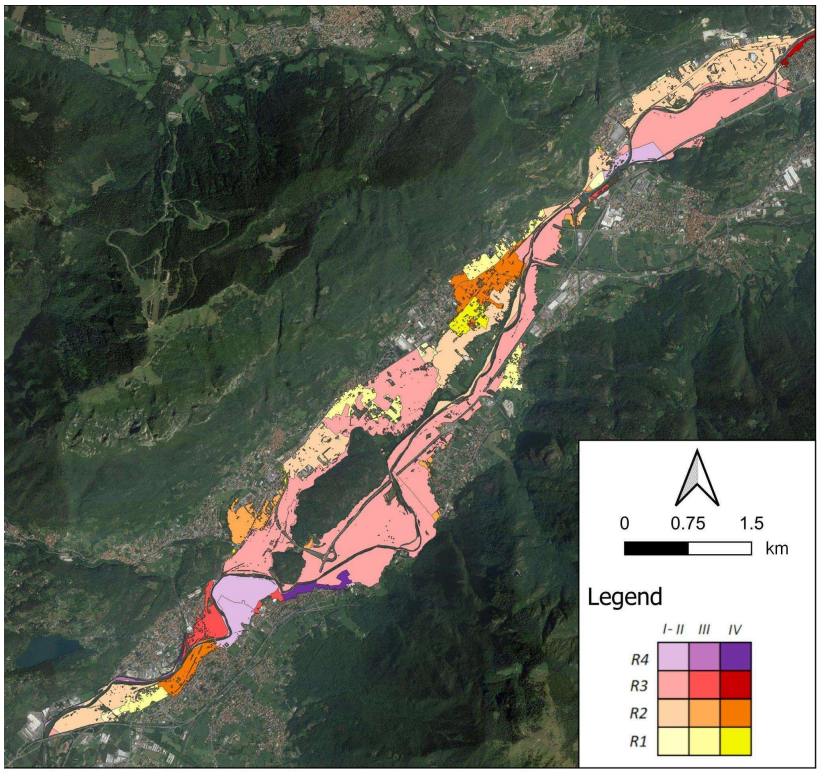

Figure 5. Risk map provided by eq.s [2], [3] and [5].

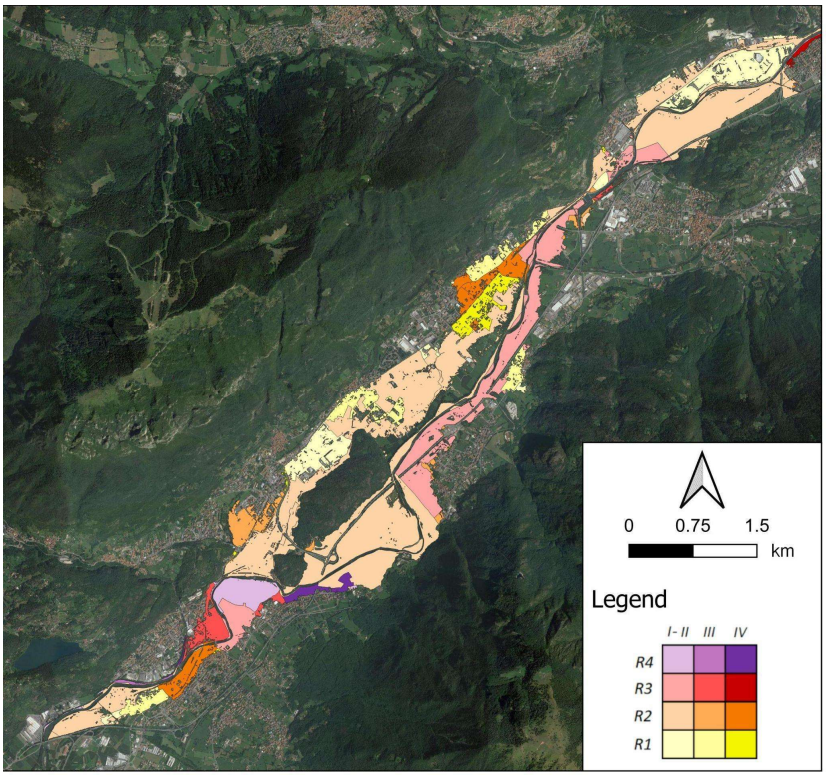

Figure 6. Risk map computed using only the information on water depth.

the solution of the SWE equations; the physical vulnerability of people, intended as combination of different possible damaging processes; the density of population on the mapped area. We believe that, in the evolutive

process foreseen by DIRECTIVE 2007/60/EC, risk mapping should be increasingly performed with rational and informative criteria like the one used in this contribution.

5. ACKNOWLEDGEMENTS

This paper benefited from discussions within the flood damage assessment research group MOVIDA coordinated by F. Ballio and D. Molinari. It was partly developed within the project Assessment of Cascading Events triggered by the Interaction of Natural Hazards and Technological Scenarios involving the release of Hazardous Substances (Grant No. 2017CEYPS8) funded by the Italian Ministry of Education, Universities and Research.

6. REFERENCES

Brunner, G. W. 2016. HEC-RAS River analysis systems user's manual. Version 5.0. Davis, CA: USACE.

Jonkman, S. N., and E. Penning-Rowsell (2008), Human instability in flood flows, J. Am. Water Resour. Assoc., 44(5), 1208–1218, doi:10.1111/j.1752-1688.2008.00217.x.

Foster, D. N., and R. Cox (1973), Stability of children on roads used as floodways, Tech. Rep. 13/73, Univ. of N. S. W., Water Res. Lab., Sidney, Australia.

Milanesi, L., and Pilotti, M., (2021). Coupling Flood Propagation Modeling and Building Collapse in Flash Flood Studies, *J. Hydraulic Engrg., ASCE*, DOI: 10.1061/(ASCE)HY.1943-7900.0001941.

Milanesi, L., Pilotti, M., Ranzi, R. (2015). A conceptual model of people's vulnerability to flood, *Water Resources Research*, 51, 182– 197.

Milanesi, L., Pilotti, M., Bacchi, B. (2016), Using web-based observations to identify thresholds of a person's stability in a flow, *Water Resources Research*, 52.

Milanesi L., Pilotti, M., Belleri, A., Marini A., and Fuchs S. (2018). Vulnerability to flash floods: a simplified structural model for masonry buildings. *Water Resources Research*, 54, 7177– 7197.

Milanesi L., and Pilotti M., (2019). A conceptual model of vehicles stability in flood flows, *Journal of Hydraulic Research*, 58(4).

Varnes, D. J. (1984), Landslide Hazard Zonation: A Review of Principles and Practices. UNESCO Natural Hazard Series, No.3, UNESCO, Paris, 63pp

©2022 IAHR. Used with permission / ISSN-L 2521-7119